AMORPHOUS and glassy CHALCOGENIDES, HIGH-TECH MATERIALS for FIBERS, MEMORIES, SENSORS, and OPTICAL SIGNAL PROCESSING

M. Frumar, B. Frumarova[1], T. Wagner, P. Nemec and M. Hrdlicka

Research Center and Dep. General and Inorg. Chemistry, University of Pardubice, Pardubice, Czech Republic, [1]Joint Lab. of Solid State Chem. of Inst. Macromol. Chemistry, Acad. Sci. of Czech Rep. and Univ. of Pardubice,

miloslav.frumar@upce.cz

Glass Tutorial Series: prepared for and produced by the **International Material Institute for New Functionality in Glass**
An NSF sponsored program – material herein not for sale
Available at www.lehigh.edu/imi

Amorphous chalcogenides:

- high optical transmissivity in IR region,
- high index of refraction,
- high optical non-linearity,
- large free volume
- large photoinduced changes of structure and physico-chemical properties

Many present and potential applications:

- **in optics and optoelectronics: lenses, microlenses, filters, coatings (antireflection, …), planar optical and integrated circuits and devices, IR lasers, acousto-optic elements, optical signal processing (light up-conversion, signal couplers, frequency mixing, amplifiers, possibly all optical computing...)**

·chemical sensing and environmental monitoring - IR, **chemical and ionic sensors (uncladed fibres -** evanescent waves, **membranes), fibers for remote sensing** –spectroscopy **(chemistry, ecology),**

·**biomedical** - X-ray and diagnostical sensors, surgical IR lasers, tissue removal, evanescent waves, in vivo measurements, eye safe radars,

·**in communications** – fibers, lasers, signal processing, ..
·**rare-earths doped chalcogenides** - **luminescence** in NIR and MID IR spectral regions: **light amplifiers, generators, eye-safe lasers, environmental and other sensors.**
·**fibres: telecommunications, power delivery, mechanical and temperature sensing, chemical and remote monitoring (medicine, in vivo spectroscopy,…)**
·**large photostructural effects: photoresists, waveguides, gratings, holography, phase-change optical and electrical memories, diffractive elements,** photoinduced dissolution and diffusion of metals

- large free volume: **photostructural** effects, **doping by Ag^+, Li^+** or other ions ⇒ **thin solid-electrolytes (batteries, ionic selective sensors**).

- **The phase-change memories** based on Ge-Sb-Te and other telluride based films - commercially applied in **DVD disks with capacity up to 50 Gb/disk, going to be increased**.
- **Ovshinsky universal (unified) memories (OUM), multilevel data storage**

1. **Preparation, bulk glasses, thin films, sputtering, pulsed laser deposition (PLD)**

- **bulk glasses – mostly direct synthesis in evacuated silica tubes → thermal quenching, annealing**

- **thin films, of binary, ternary or multinary systems**, vacuum thermal evaporation (TE) is not suitable ⇒ **fractional evaporation or nonstoichiometry**.

possible solution: (PLD). Evaporation by (ns or fs) pulses of high intensity and energy, excimer lasers emitting in UV region, (e.g. KrF, 248nm, ~5eV ≈ 480kJ/mol., ~10^8 – 10^9 **W/cm²**)

→ **nearly any material can be evaporated**,

every pulse evaporates all components, independently on their vapor pressure.

The stoichiometry is often preserved.

The **kinetic energy** (temperature) of evaporated particles **~ keV** - the reactions among the particles or fragments are quicker.

⇒ the **structure** **of some ablated films can be closer to the structure of target glass** -

⇒ new materials are obtained (contrary to thermal evaporation).

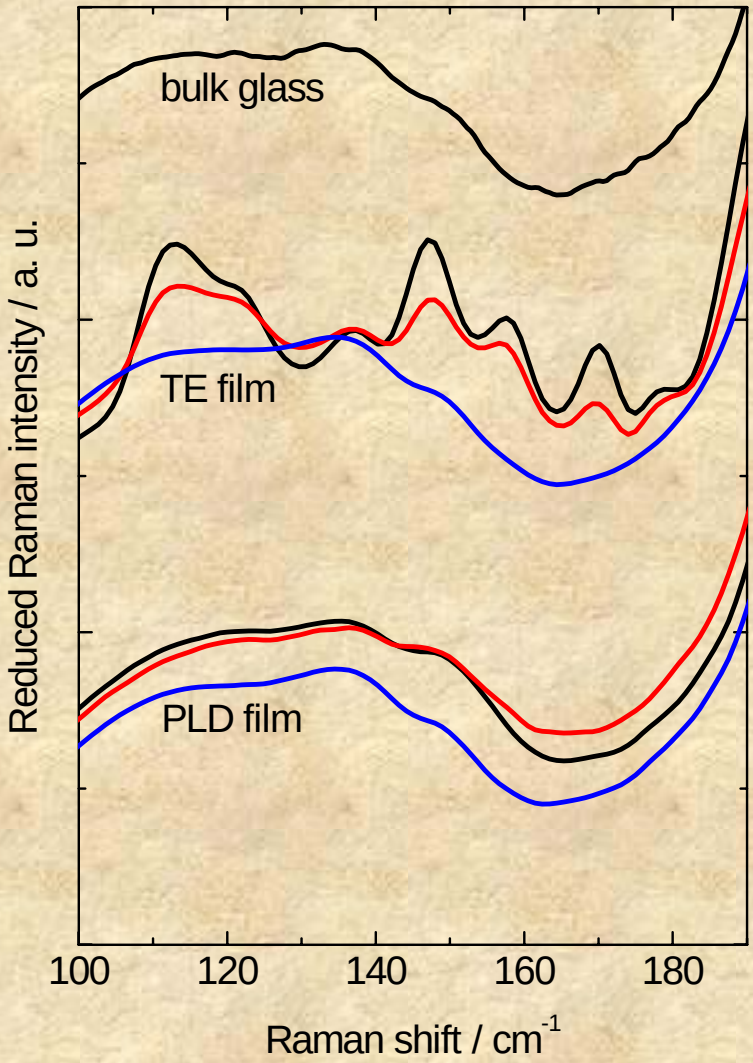

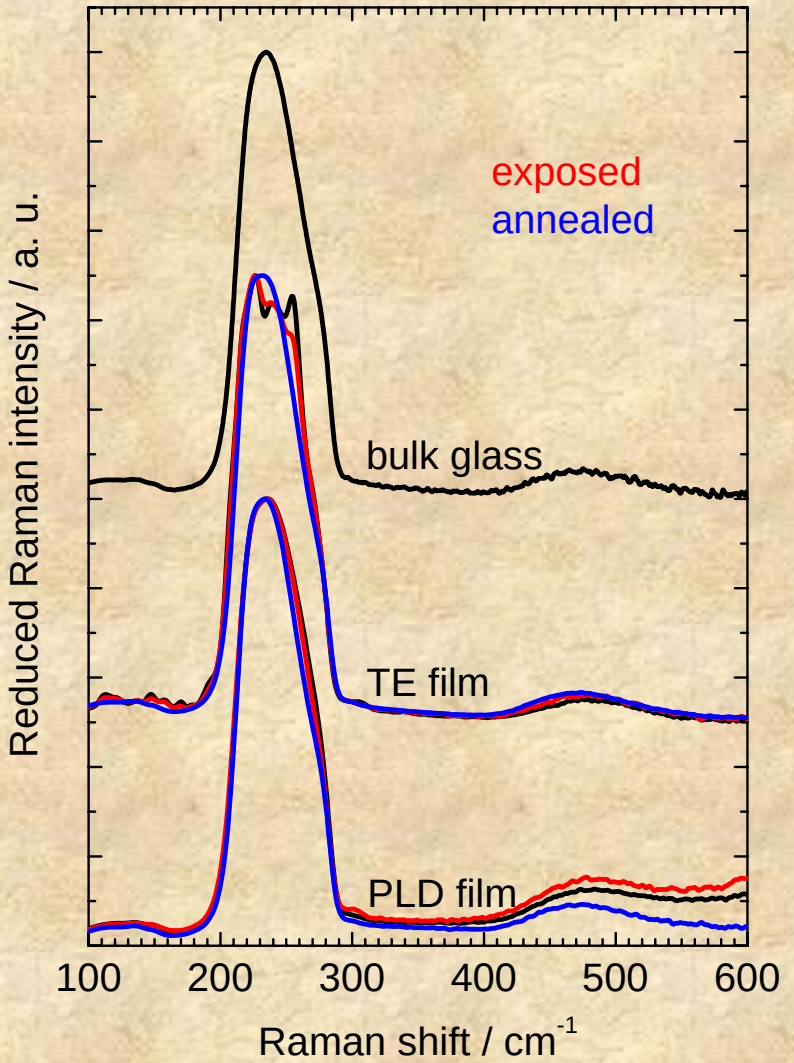

Raman spectra of bulk As_2Se_3 glass and As-Se thin films

The PLD films of As_2Se_3 contain **less 'wrong' As-As and Se-Se bonds** and **As_4Se_4, As_4Se_3, Se_8 or Se_n** particles.

⇒ **probably due to higher kinetic energy** of the plasma-plume particles: **enables their interaction** (Eqs. 1-3) ⇒ densities of **As_4Se_4, As_4Se_3, Se_n are lowered, e.g.**

$$As_4Se_4 + (2/n)\,Se_n = 2\,As_2Se_3 \quad (1)$$
$$As_4Se_3 + (3/n)\,Se_n = 2\,As_2Se_3, \quad (2)$$
$$|As\text{-}As| + |Se\text{-}Se| = 2|As\text{-}Se| \quad (3)$$

In **As-S system**: during evaporation - thermal dissociation, change of composition

$$2As_2S_3 = As_4S_4 + S_2, \quad (4)$$

para-realgar (**As_4S_4**) is formed at high temperatures

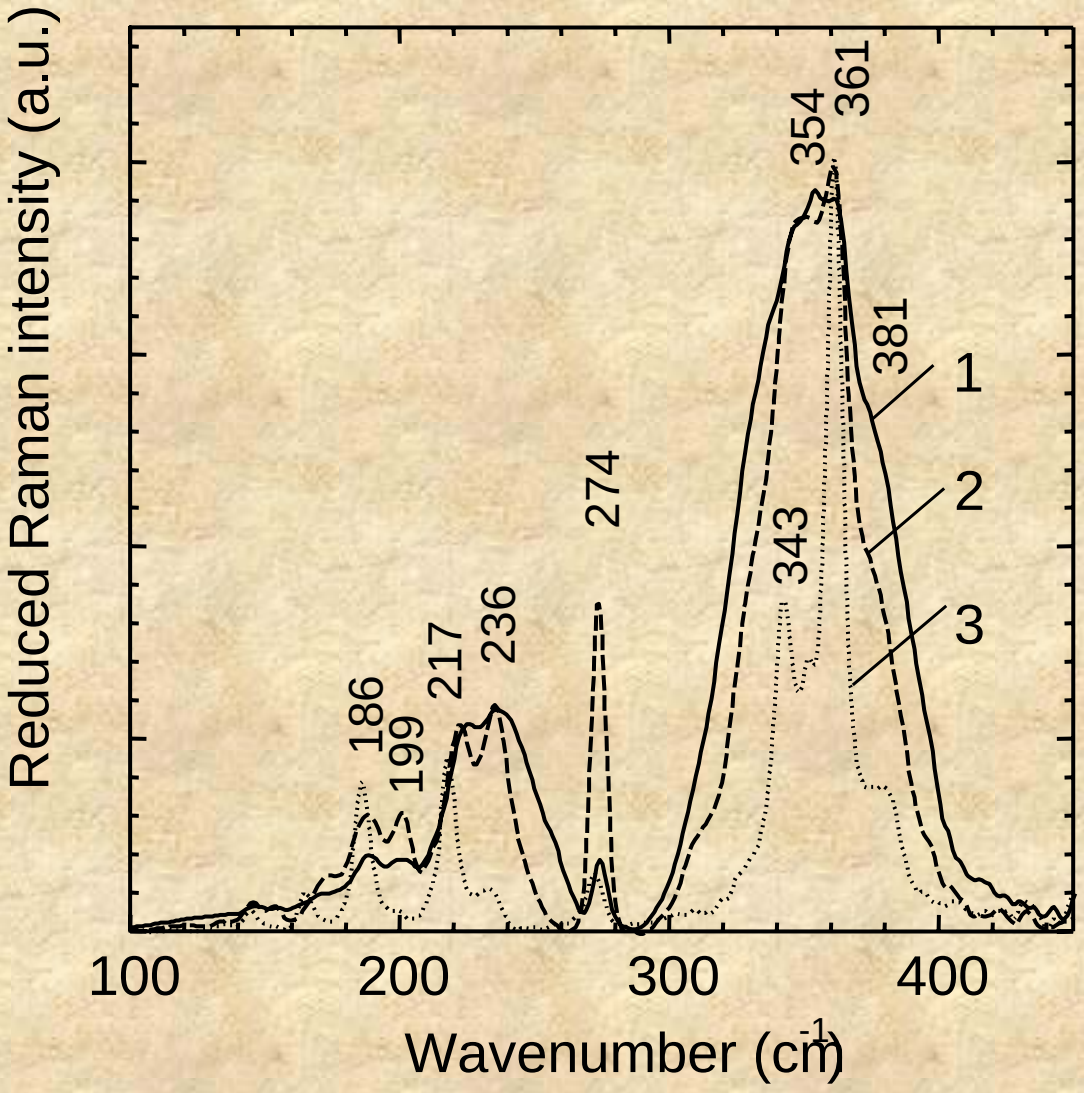

PLD As_2S_3 → ~$As_{50}S_{50}$

1 as-evap.
2 expos.
3 anneal.

The photoinduced processes are enabled by relatively large free volume. It is inversely proportional to the ω

$$\omega = |M - S|\,\delta = |M - S|\left[\rho \frac{\sum(A_i x_i/\rho_i) - \sum(A_i x_i/\rho)}{\sum A_i x_i}\right] \qquad (5)$$

low coordination number of chalcogens (mostly $N_c \cong 2$), and of pnictides, (e.g. $N_c(As) \cong 3$).

Irreversible photoinduced changes:

homogenization, chemical reactions among fragments formed by dissociation during evaporation, e.g.

$$As_4S_4 + S_2 = 2As_2S_3 \qquad (6)$$

Exposure increases the rates of synthetic reactions, also some photolytic reactions.

The reversible photoinduced changes are connected with changes of local bonding configurations.

For As-S, As-Ga-S, As-Sb-S, and Sb_2S_3, Ge-Sb-S films and bulk glasses, a model has been proposed.

$$2|As-S| \xleftrightarrow{h\nu_i, I_i} |As-As| + |S-S| \qquad (7)$$

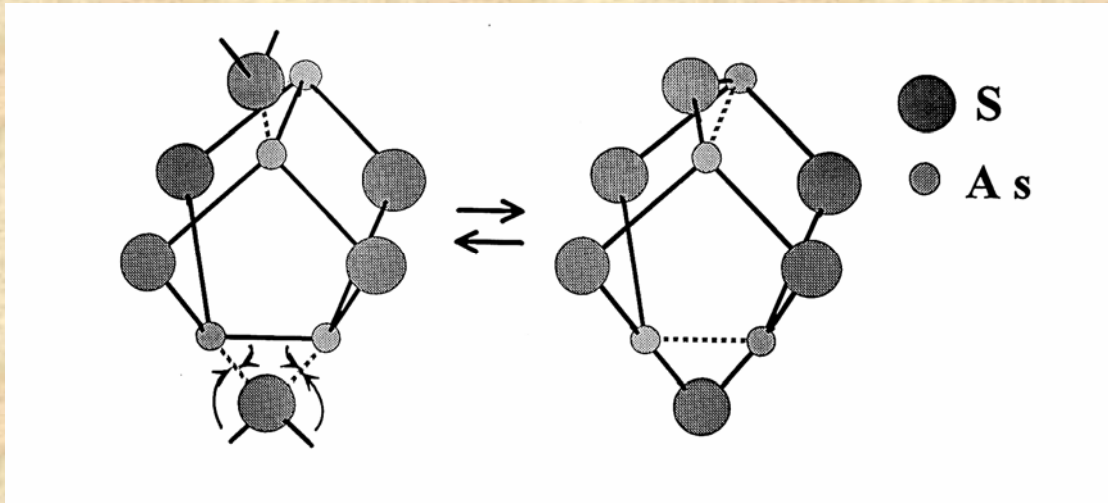

supported by Raman spectroscopy results, As_2S_3

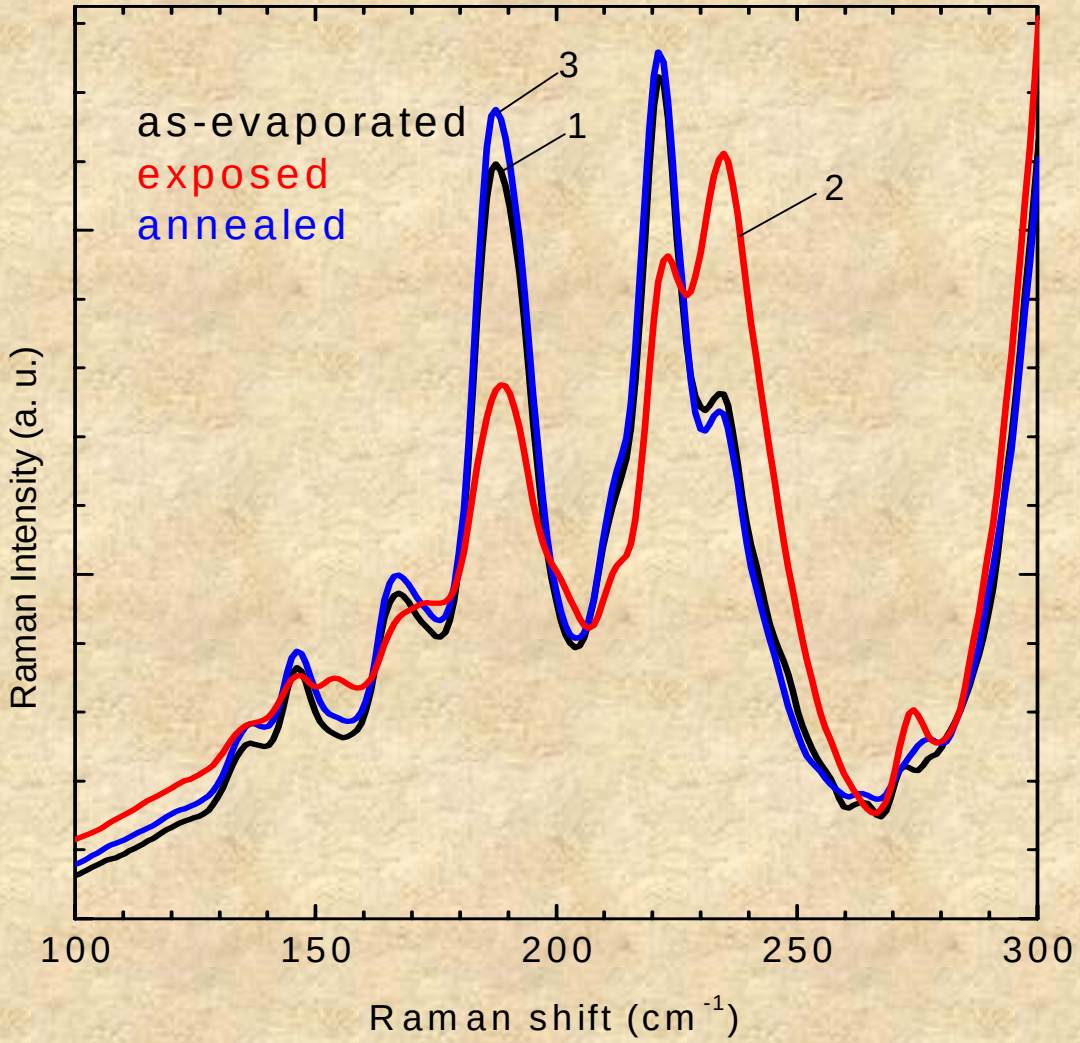

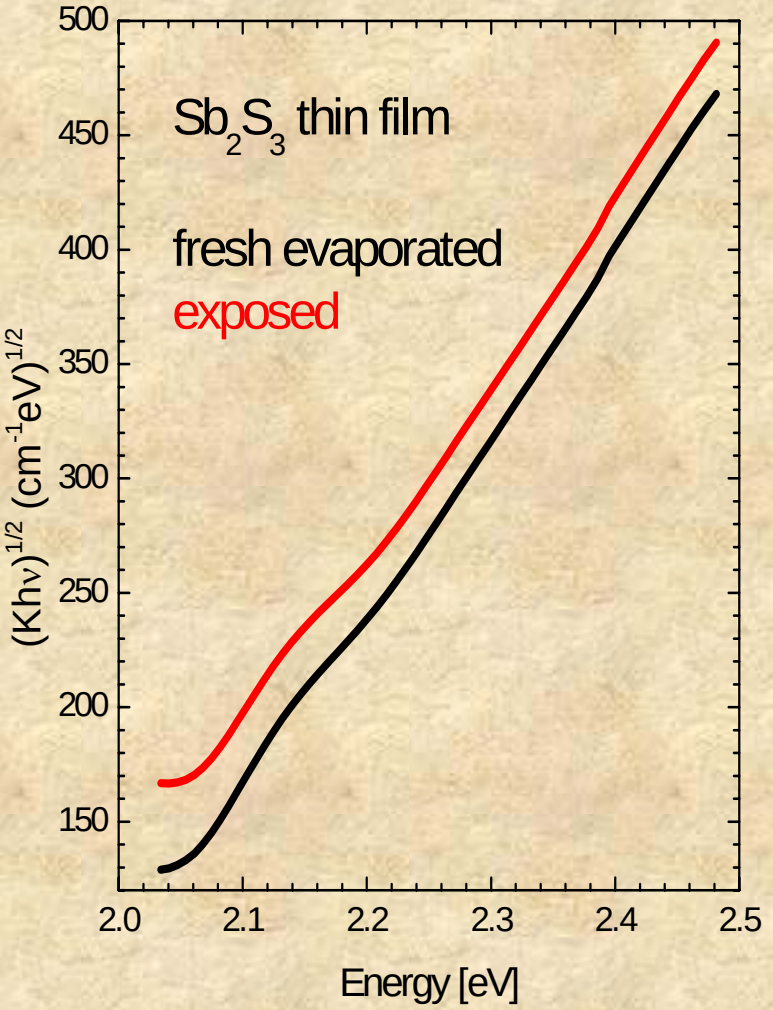
Sb2S3 thin film
fresh evaporated
exposed
(Khν)1/2 (cm-1eV)1/2
Energy [eV]
500
450
400
350
300
250
200
150
2.0
2.1
2.2
2.3
2.4
2.5

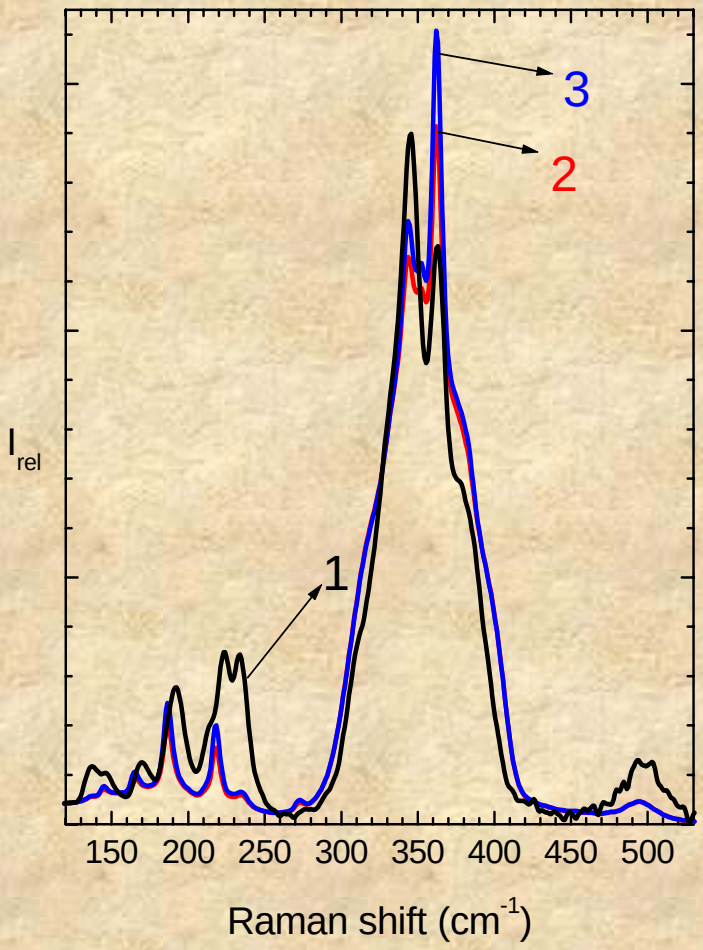

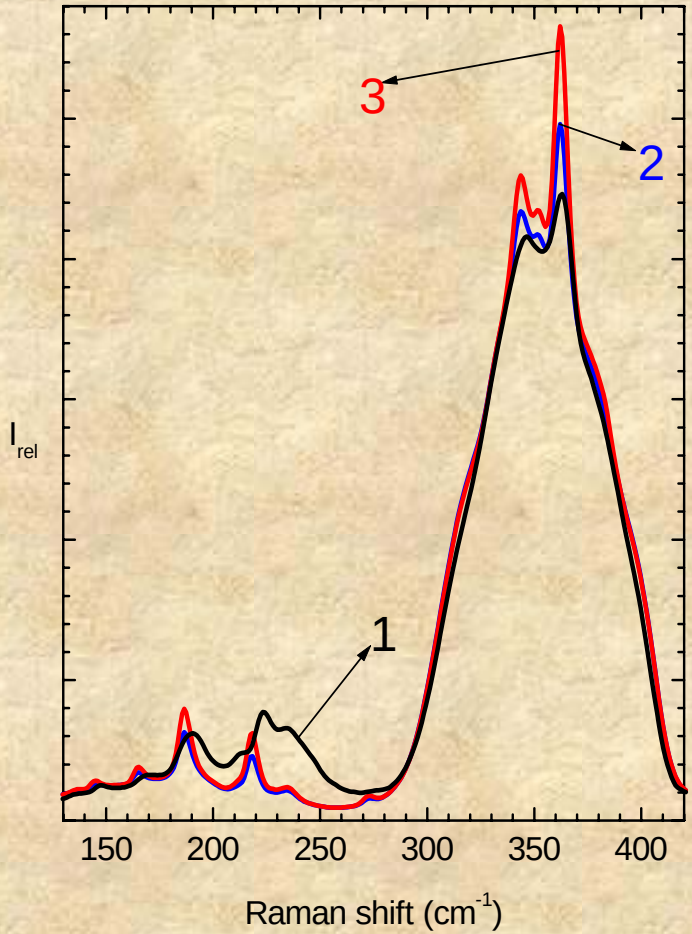

1. $As_{42}S_{58}$ fresh evaporated film
2. mixture of $0.85As_{40}S_{60}+0.15As_4S_4$
3. mixture of $0.8As_{40}S_{60}+0.2As_4S_4$

1. $As_{42}S_{58}$ annealed film
2. mixture of $0.9As_{40}S_{60}+0.1As_4S_4$
3. mixture of $0.85As_{40}S_{60}+0.15As_4S_4$

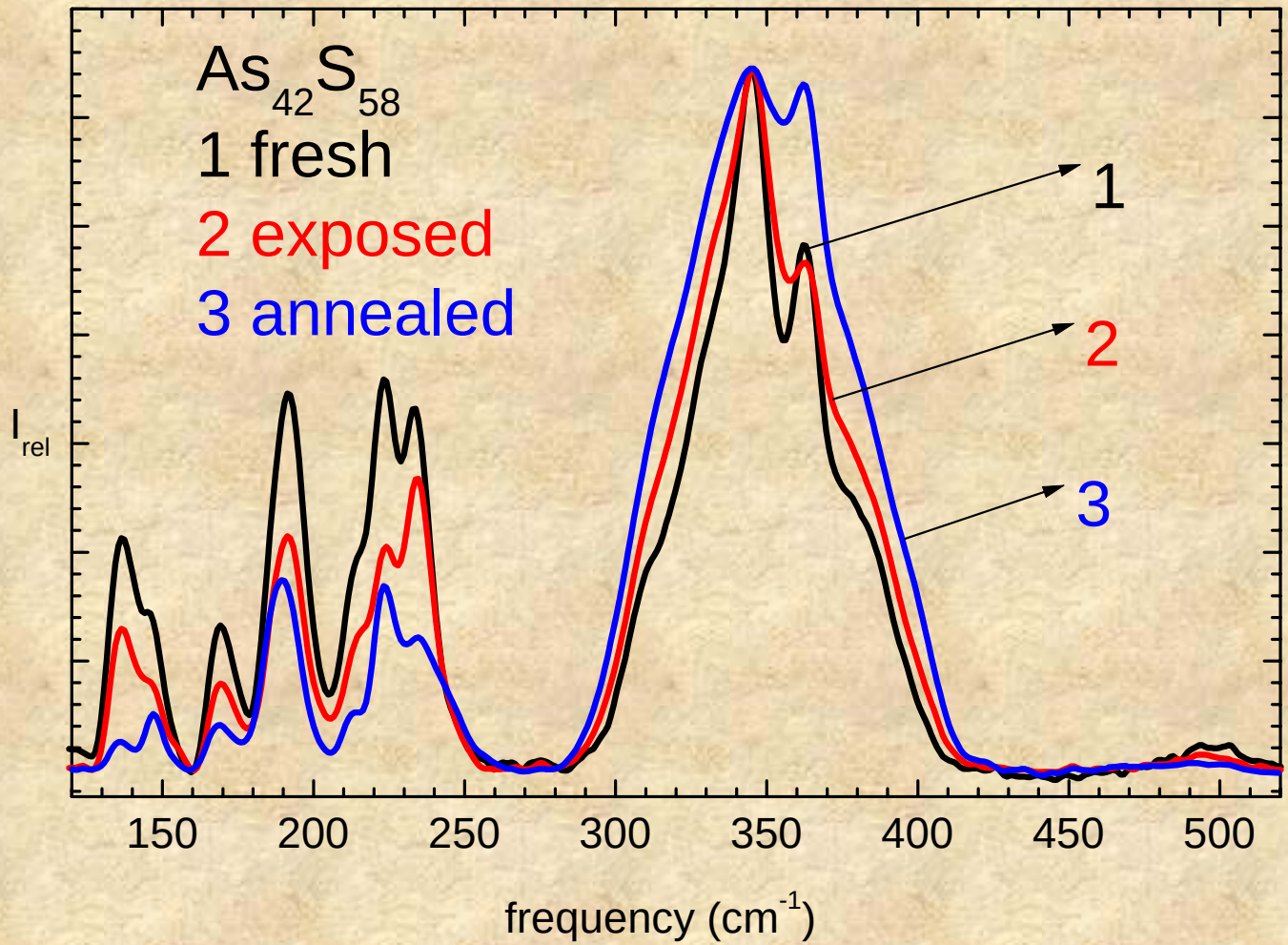
As42S58
1 fresh
2 exposed
3 annealed
1
2
3
Irel
150
200
250
300
350
400
450
500
frequency (cm-1)

Dependence of $(Kh\nu)^{1/2}$ on photon energy in $As_{40}S_{60}$ films.
K is the absorption coefficient (cm^{-1}), $h\nu$ is photon energy

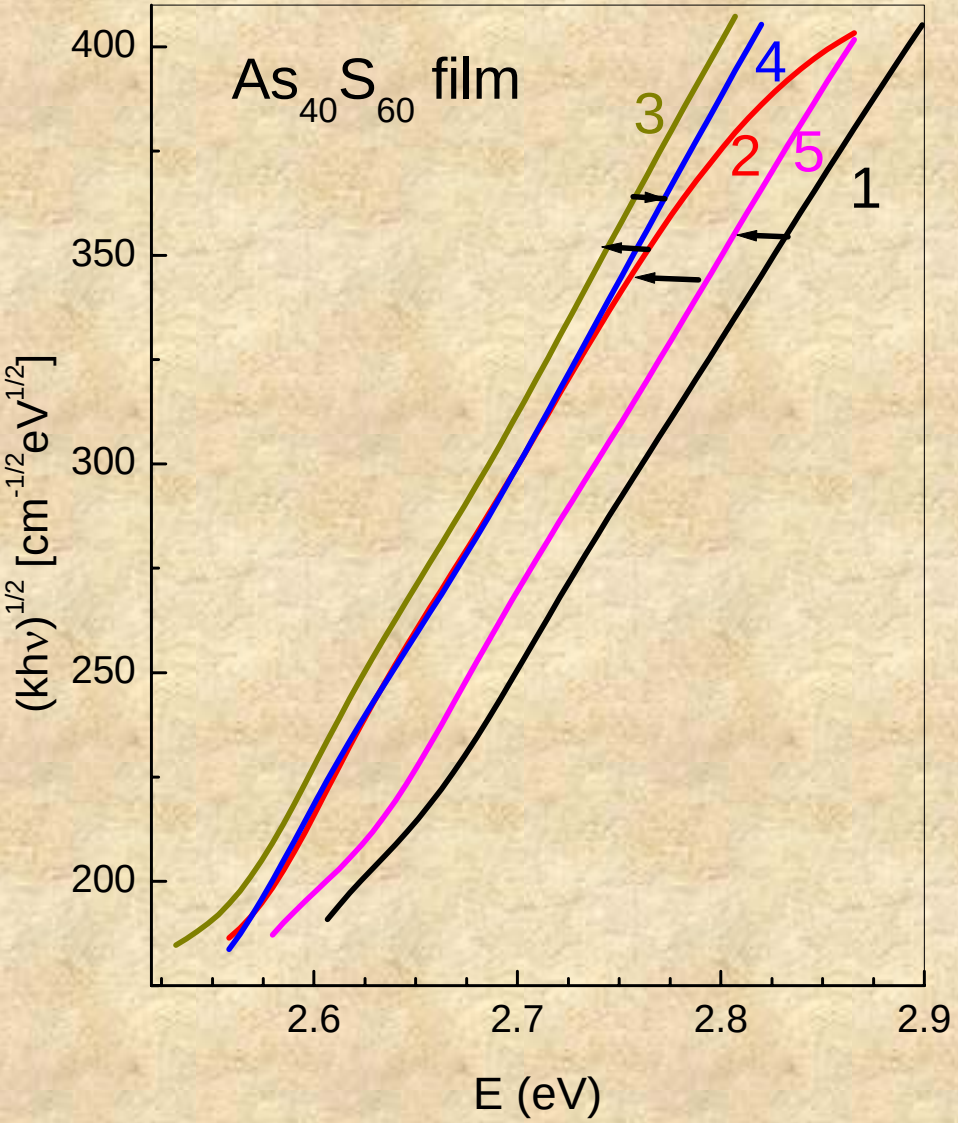

1 fresh evaporated film,

2 fresh → annealed

3 fresh → annealed → exposed

4 fresh → annealed → exposed → annealed

5 fresh → exposed

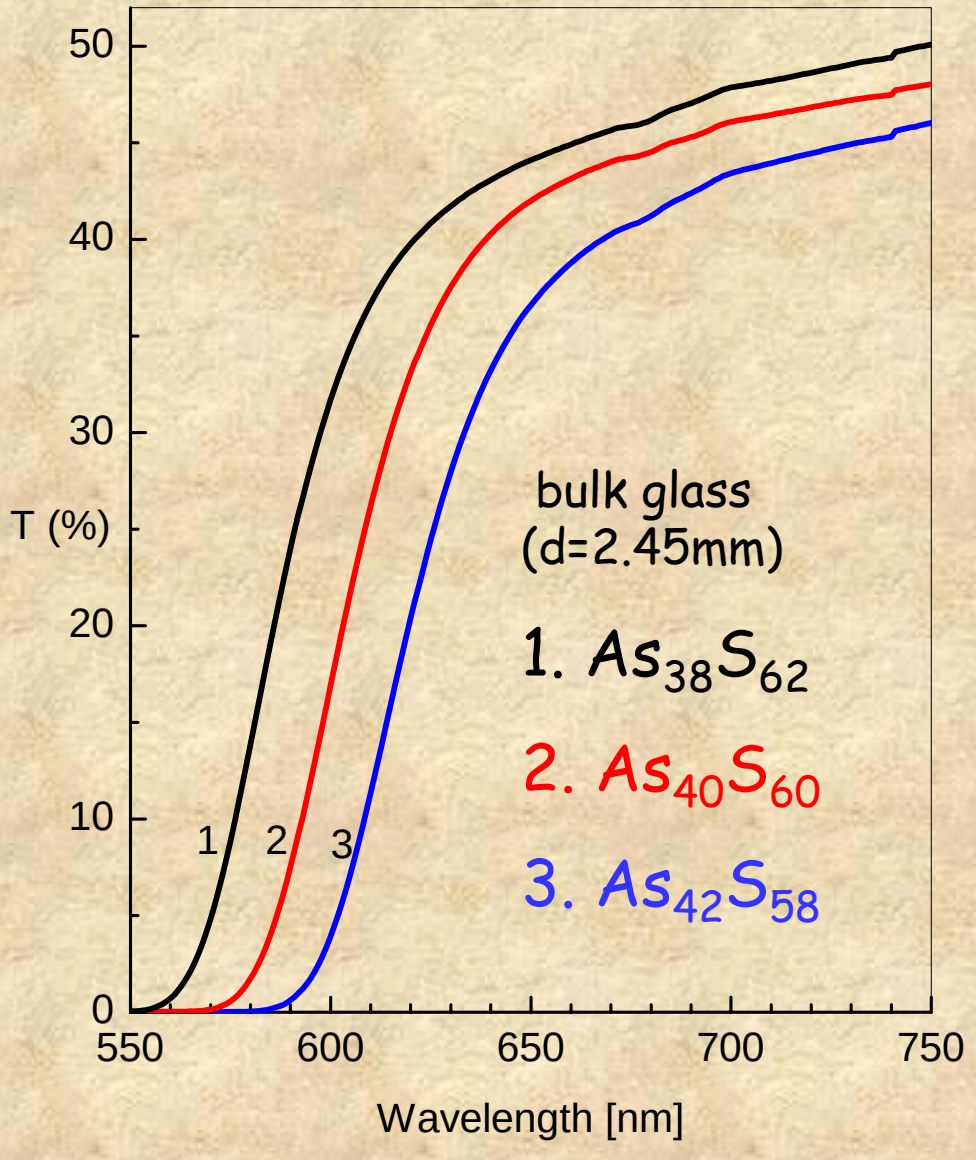
50
40
30
20
10
0
T (%)
550
600
650
700
750
Wavelength [nm]
1
2
3
bulk glass
(d=2.45mm)
1. As38S62
2. As40S60
3. As42S58

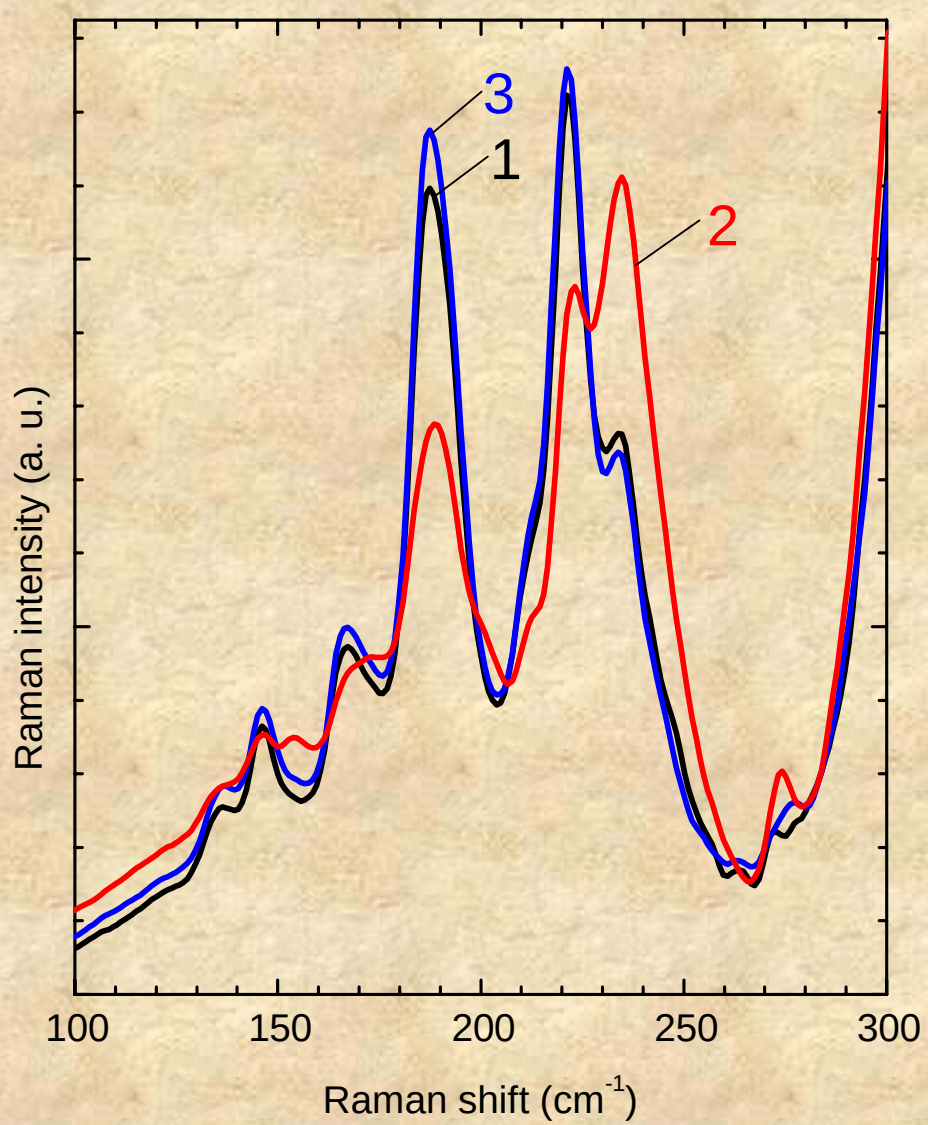

Reduced Raman spectra of thin films (d = 1000 nm) of $95As_2S_3.5GaS$.

1: annealed film, *2:* film exposed after annealing, *3:* film was annealed after exposure.

The change of amplitudes corresponds to reversible structural changes,

the band (235 cm^{-1}) with increased amplitude corresponds to As-As vibrations

In PLD films of As_2Se_3, **the exposure increases the index of refraction**, and following **annealing ⇒ the index of refraction decreases** ↔ **densification and thermally-induced expansion** of the amorphous layers.

Index of refraction, n, is different for bulk glasses, PLD and TE films, Δn can be larger for PLD films

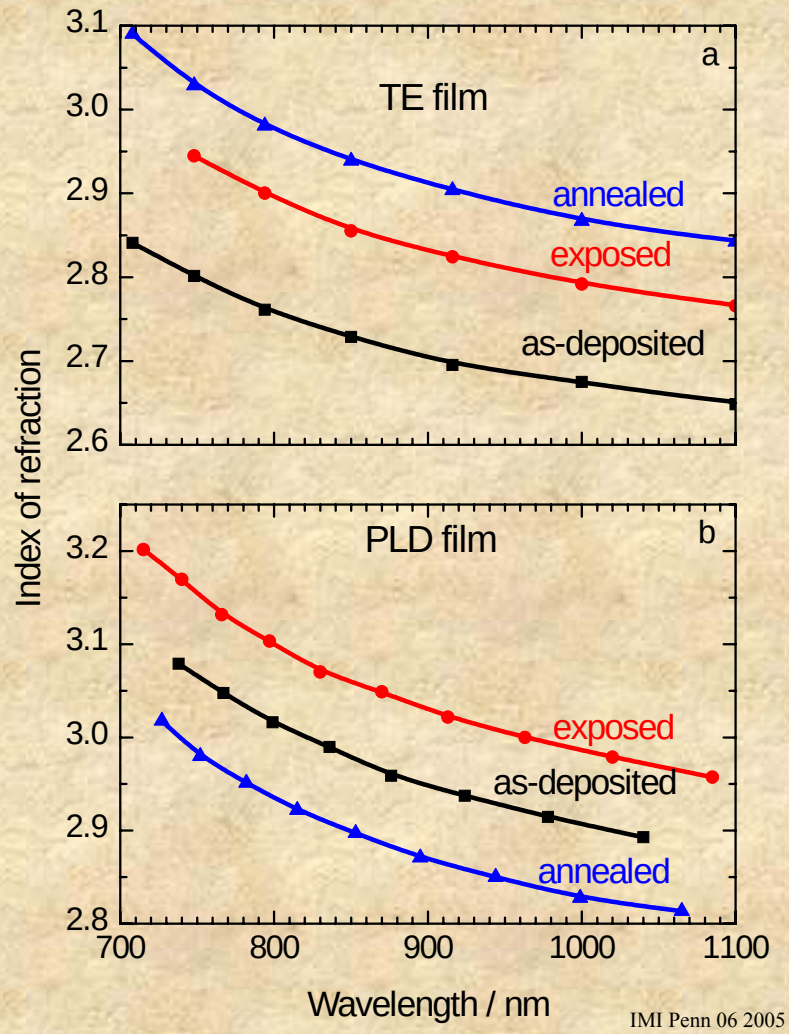

Nonlinear properties → signal processing

The refractive index, $n = n_o + n_2 \langle E^2 \rangle$, n_0 and n_2 do not depend on intensity of light, $n_0 >> n_2$.

The $\langle E^2 \rangle$ is the mean square of electric field. The fast part of nonlinear index of refraction, n_2, is connected with nonlinear electron polarizability, P_{NL}

$$P = \chi^{(1)}E + P_{NL} , \qquad (8)$$

$$P_{NL} = \chi^{(2)}E^2 + \chi^{(3)}E^3. \qquad (9)$$

The P is polarizability, $\chi^{(1)}$ is the linear optical susceptibility, $\chi^{(2)}$ and $\chi^{(3)}$ are second- and third-order non-linear optical susceptibilities, respectively.

The linear optical susceptibility of isotropic medium is given by relation

$$\chi^{(1)} = (n^2-1)/4\pi \ . \qquad (10)$$

The dependence of $(n^2-1)^{-1}$ vs. $(\hbar\omega)^2$ is often linear and this dependence can be described by single oscillator formula of Wemple and DiDomenico

$$n^2(\omega) - 1 = E_0E_d/(E_0^2 - (\hbar\omega)^2), \qquad (11)$$

where E_0 is single oscillator energy, E_d is so called dispersion energy and $\hbar\omega$ is energy of light.

for long wavelengths, $\chi^{(1)} = E_d/4\pi E_0$.

For optically isotropic glasses, the $\chi^{(2)}$ is zero.

The $\chi^{(3)}$, as a dominant nonlinearity in all glassy materials, produced by excitation in the transparent frequency region well below the band gap, E_g^{opt}.

Only $\chi^{(3)}$ contributes to the nonlinear behavior.

IMI Penn 06 2005 22

For the region far from resonance (Miller's rule)

$$\chi^{(3)} \approx A(\chi^{(1)})^4 \times 10^{-10} \text{ esu.} \qquad (12)$$

For single oscillator (Wemple and DiDomenico)

$$\chi^{(1)} = \frac{E_d E_0}{4\pi(E_0^2 - (\hbar\omega)^2)} \qquad (13)$$

$$\chi^{(3)} = [E_d E_0 / 4\pi(E_0^2 - \hbar\omega)^2]^4 \times 10^{-10}, \text{ (esu).} \qquad (14)$$

E_0 is single oscillator energy, E_d is dispersion energy.

For $\hbar\omega \rightarrow 0$,

$$\chi^{(3)} = \frac{A}{(4\pi)^4}\left(\frac{E_d}{E_0}\right)^4 = \frac{A}{(4\pi)^4}\left(n_0^2 - 1\right)^4 = 4.02\times10^{-15}(E_d/E_0)^4 \text{ (esu)} \qquad (15)$$

$A \cong 1.7 \times 10^{-10}$ (for $\chi^{(3)}$ in esu) and n_0 is the linear index of refraction.

The values of n_0 are high in chalcogenides and are significantly higher in PLD films in comparison with TE films.

The $\chi^{(3)}$ →**also higher**. **Using the formula (15) :**

As_2S_3 glass: $\chi^{(3)}$ = (1.48 – 2.2) x10^{-12} esu
GeS_2 glass, $\chi^{(3)}$ = 1x10^{-12} esu,
SiO_2 glass, $\chi^{(3)}$ = 2.8x10^{-14} (esu) for λ= 1900 nm.

larger $\chi^{(3)} \Rightarrow$ lower necessary power and shorter the interaction lengths $\Rightarrow$

Chalcogenides - promising candidates for optical switching and other applications

Silver containing chalcogenide glasses, photodoping.

Exposure controlled dissolution of Me and diffusion of Me^+

Model,
Applications:

- Lithography
- Diffractive optical elements, (diffractive gratings,…)
- IR components, waveguides, microlens arrays, ...)
- Optical storage
- Nonlinear optics

Phase diffraction gratings

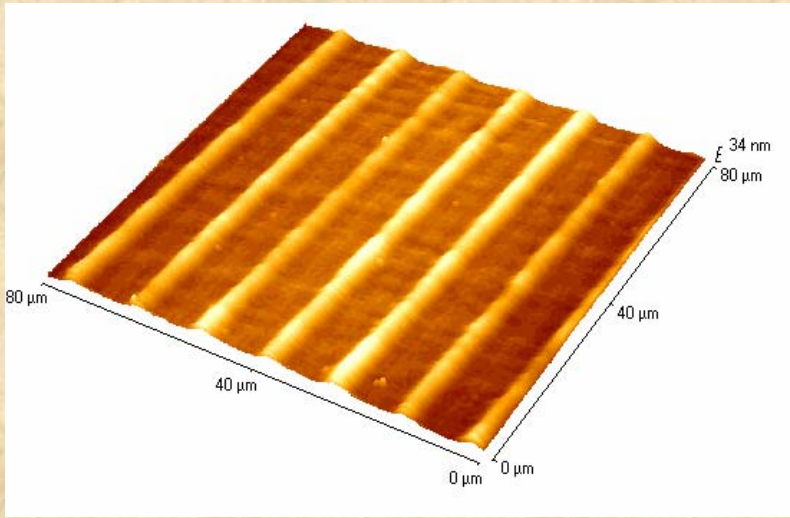

Microlenses arrays

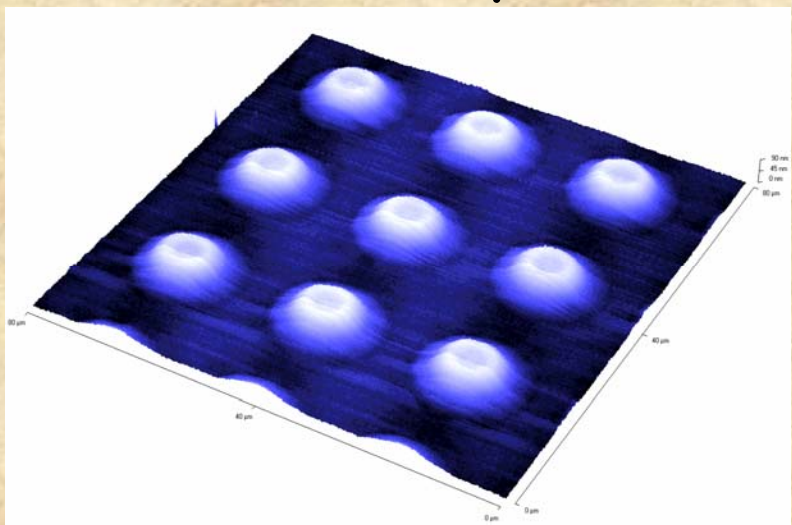

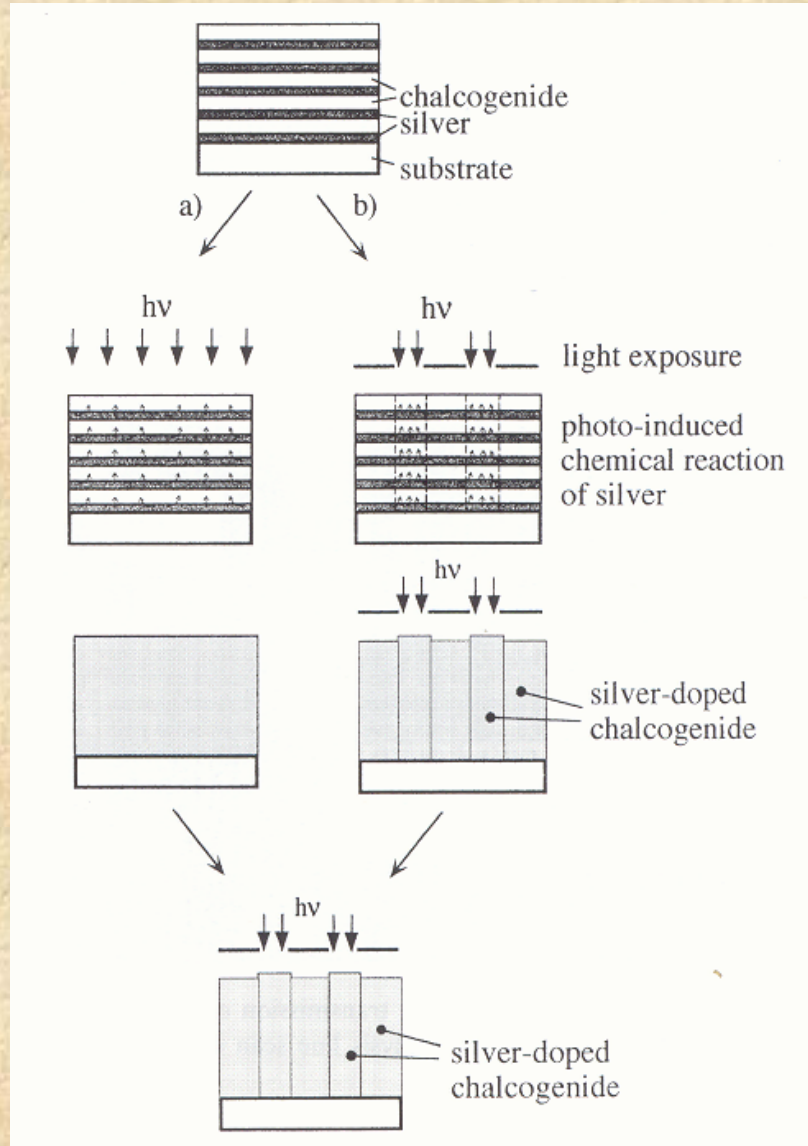

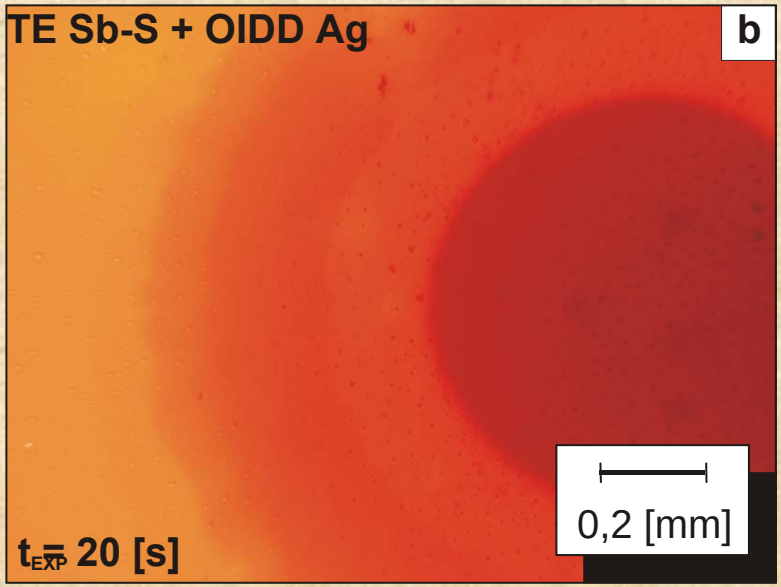
TE Sb-S + OIDD Ag
b
0,2 [mm]
t_EXP 20 [s]

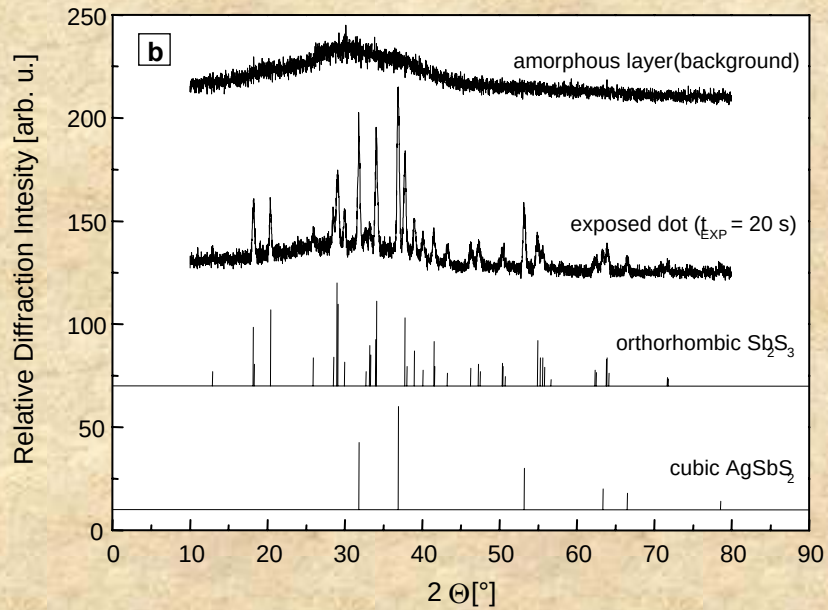
b
amorphous layer(background)
exposed dot (t_EXP = 20 s)
orthorhombic Sb2S3
cubic AgSbS2
Relative Diffraction Intesity [arb. u.]
2 Θ[°]
0
50
100
150
200
250
0
10
20
30
40
50
60
70
80
90

Eutectic tellurides, recently:

$Sn_{16}Te_{84}$, $In_{13}Te_{87}$, $Sb_{11}Te_{89}$.

Melting t ≅ 400-420°C

Bulk samples- **crystalline**

ablated films – **amorphous, good optical transmittance up to 18 μm,** untill now- many droplets

Excimer laser pulses – crystallization,

prevailing Te crystals

$Sn_{16}Te_{84}$

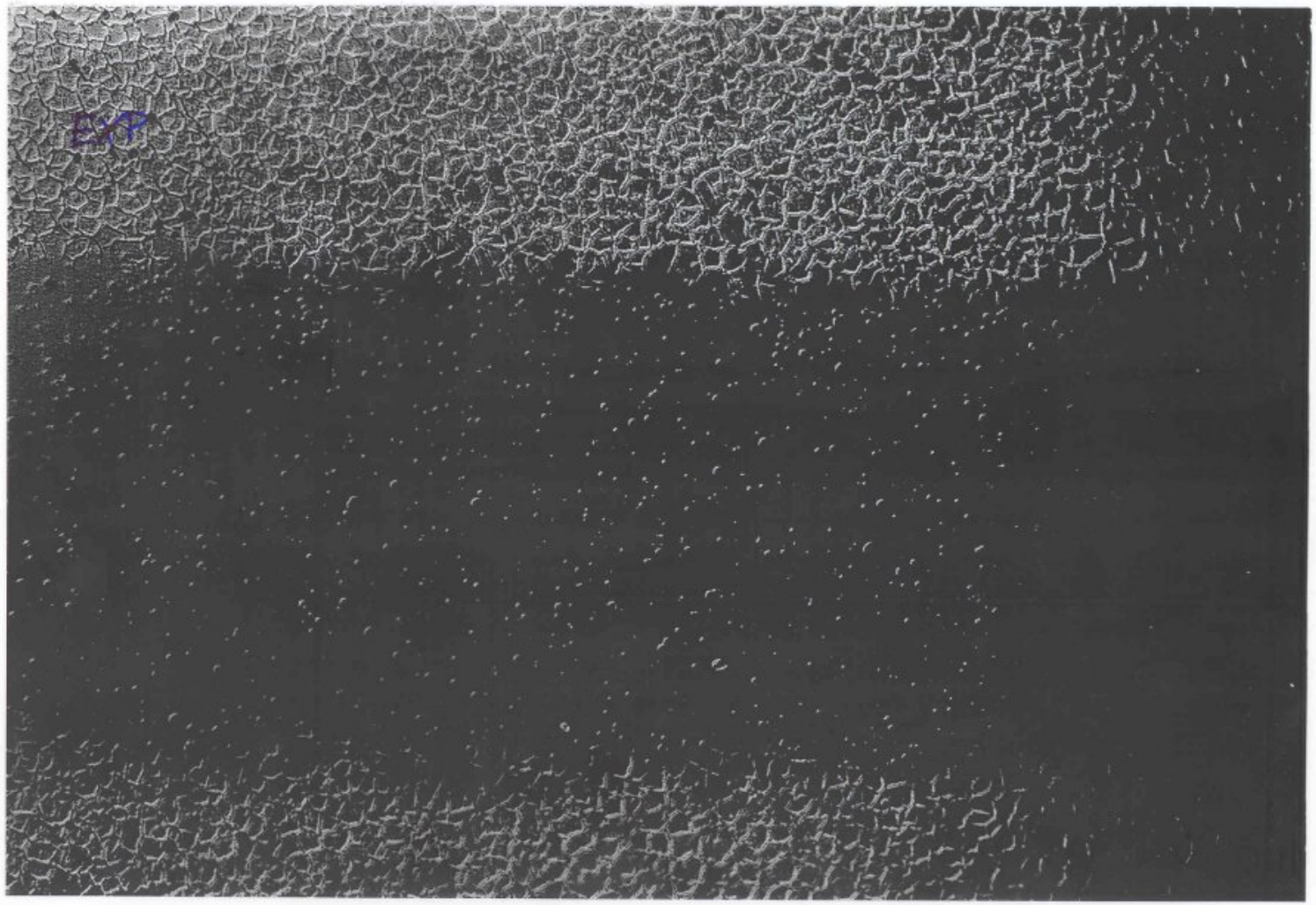

RE^{3+} doped glasses

Intensive luminescence in NIR and MID-IR part of spectrum

Low phonon energy: the number of phonons to bridge the energy gap between the electron levels of RE ion, ΔE, is large →

multiphonon relaxation rate is low !

The non-radiative decay rate, ω_p, due to multiphonon relaxation, Miyakawa-Dexter:

$$\omega_p = \omega_0 \exp(\alpha \Delta E/\hbar\omega), \qquad (16)$$

α = ln(p/g) - 1, p = $\Delta E/\hbar\omega$, g is the electron-phonon coupling strength, and ω_o is a host dependent constant.

For a high luminescence efficiency also:

high index of refraction,

higher values of spontaneous emission probabilities,

large emission cross-sections of radiative electron transitions between energy levels of RE^{3+} ions.

luminescence spectra

excitation wavelength 1064 nm

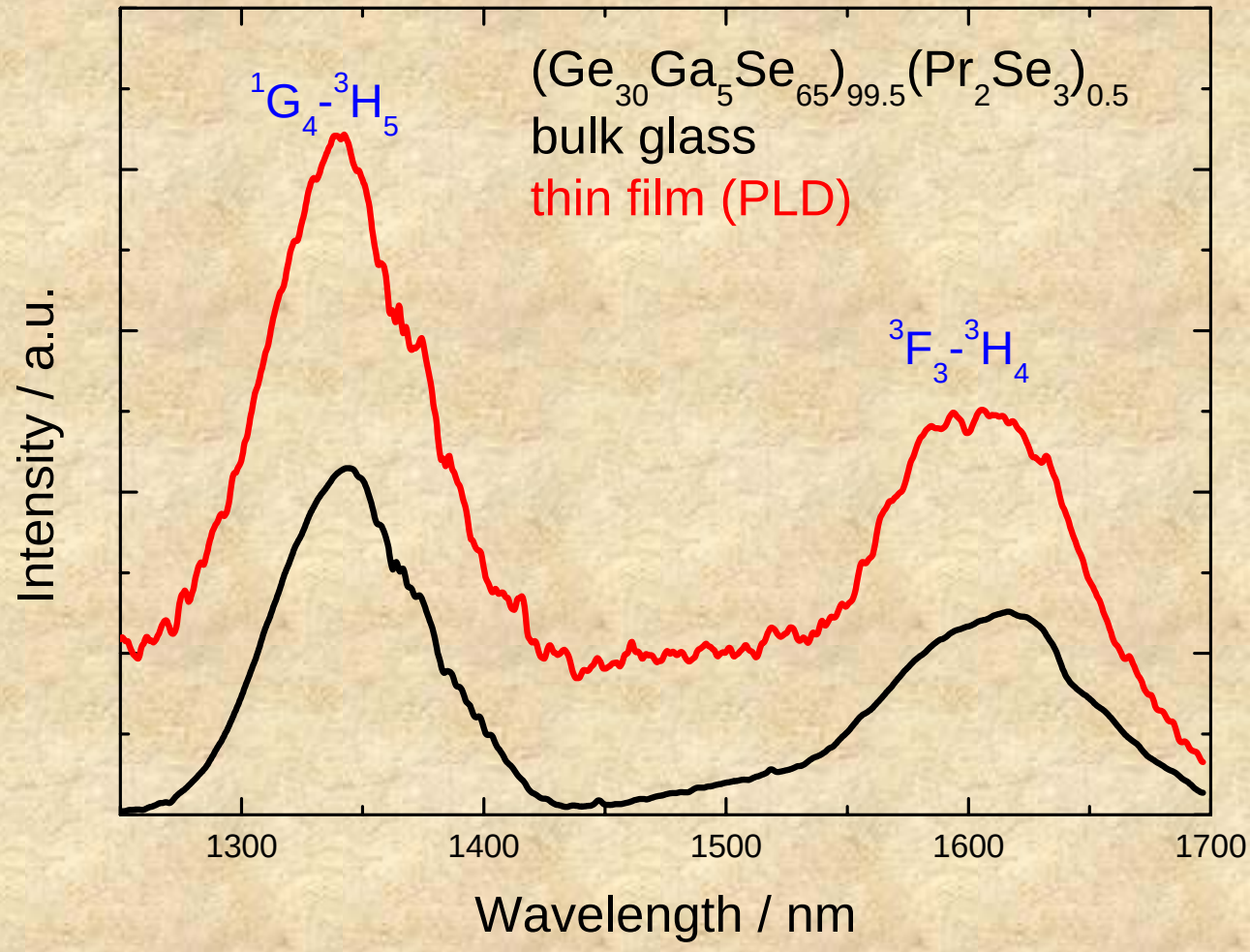

luminescence spectra

excitation wavelength 1064 nm

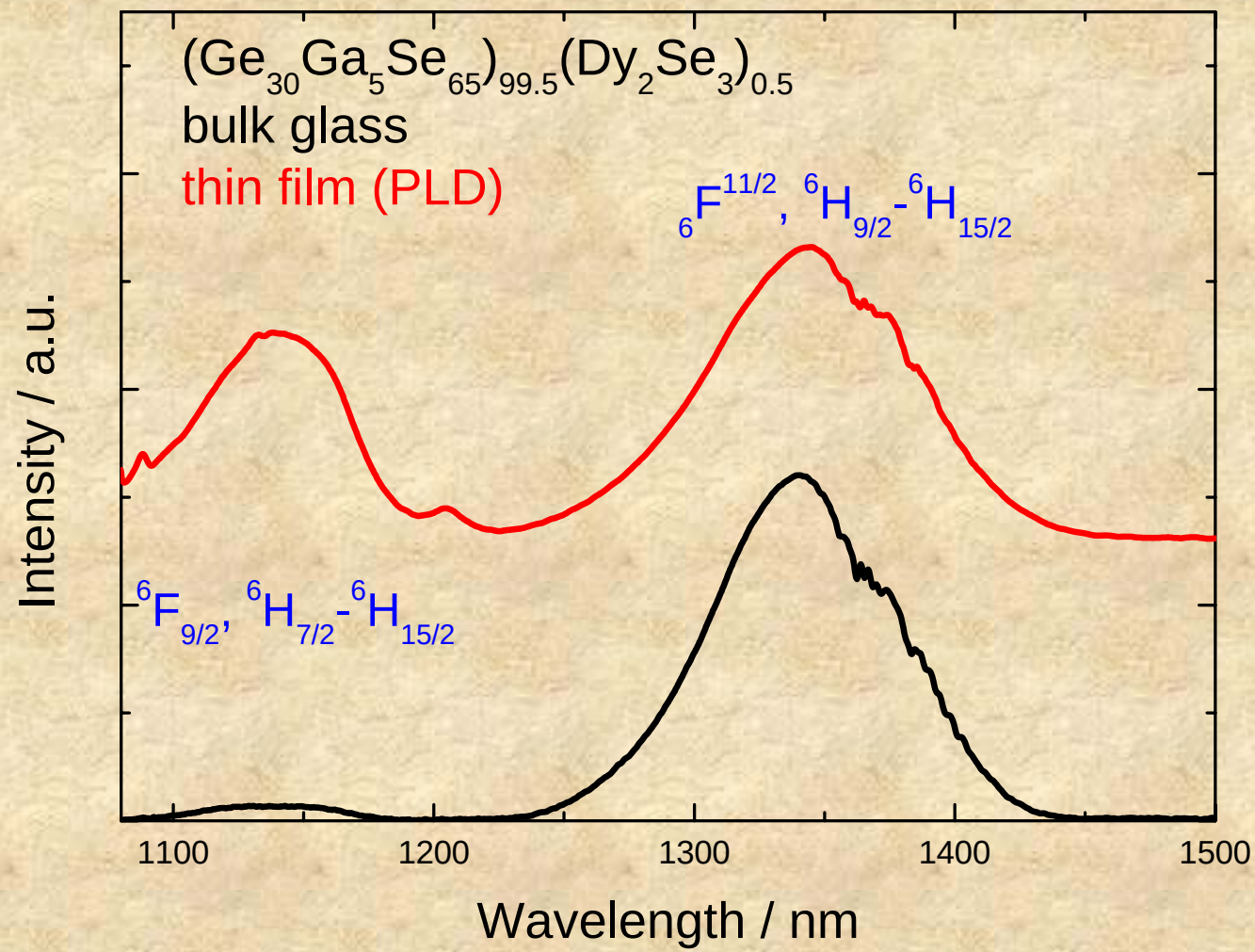

2) $(As_2S_3)_{0.95}(In_2S_3)_{0.05}$ doped by Sm

The luminescence, near IR region (bands near 1130, 1240, 1290, and 1490 nm), typical for Sm^{3+} ions;

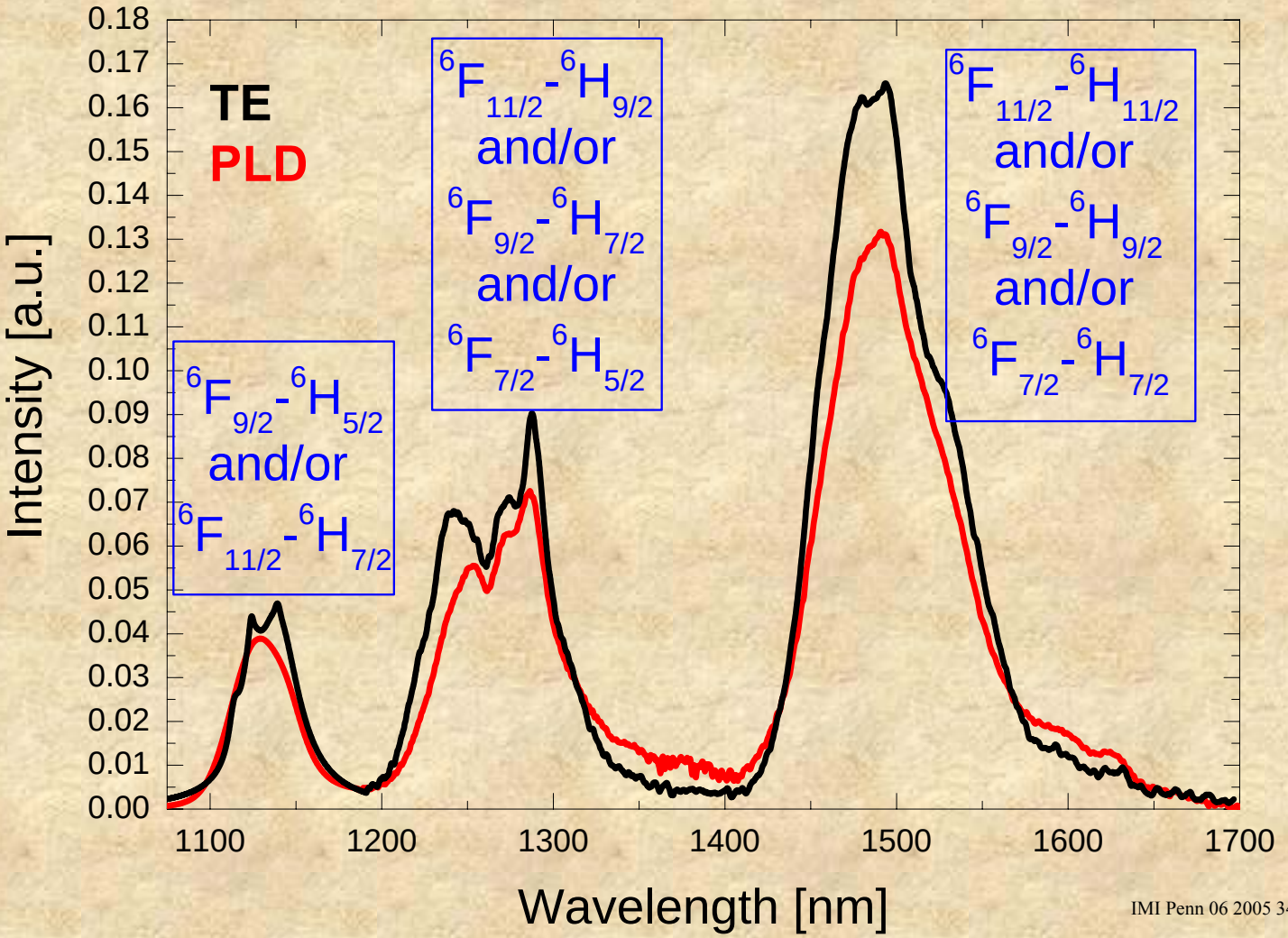

Judd-Ofelt intensity parameters were evaluated the measured oscillator strengths

$$f_{cal}\left((S,L)J,(S',L')J'\right)=$$

$$=\frac{8\pi^2 m\upsilon}{3h(2J+1)}\left[\frac{\left(n^2+2\right)^2}{9n}\sum_{t=2,4,6}\Omega_t\left|\left\langle (S,L)J\left\|U^{(t)}\right\|(S',L')J'\right\rangle\right|^2\right] \qquad (17)$$

f_{cal} are calculated oscillator strengths, h is Planck's constant, m is electron mass, υ is mean wavenumber of the absorption band, *J is the ground-state total angular momentum of Sm^{3+} (J=5/2)*, n is the refractive index of the material, *Ω_t are the Judd-Ofelt phenomenological intensity parameters and the* $\left\langle (S,L)J\left\|U^{(t)}\right\|(S',L')J'\right\rangle$

are the reduced matrix elements of the tensor operator, $U^{(t)}$ of rank t.

Values of the Judd-Ofelt intensity parameters, e. g. for Sm^{3+} ions in Ge-Ga-Se glasses:

Ω_2 = 7.423 x 10^{-20} cm^2, Ω_4 = 14.428 x 10^{-20} cm^2, Ω_6 = 6.428 x 10^{-20} cm^2.

From the Judd-Ofelt intensity parameters, Ω_t:

The spontaneous transition probability A of an electric-dipole transition:

$$A[(S,L)J;(S',L')J'] = \frac{64\pi^4 e^2 n}{3h(2J+1)\bar{\lambda}^3}\left[\frac{(n^2+2)^2}{9}\right] \times \sum_{t=2,4,6} \Omega_t \left|\left\langle (S,L)J \| U^{(t)} \| (S',L')J' \right\rangle\right|^2 \qquad (18)$$

e is the electron charge and $\bar{\lambda}$ *is the average wavelength of the transition.*

The value of A is high in studied glasses.

Conclusion:

Chalcogenide glasses and films posses many interesting properties applicable in optics, optoelectronics, data storage, in chemistry, medicine and biology.

Acknowledgements

The support of Ministry of Education of the Czech Republic under the projects LC 523, KONTAKT ME 690, 002167501, is highly acknowledged.

Thank you for invitation and your kind attention